Theoretical and Experimental Investigation of the Energetics of Cis−Trans Proline Isomerization in Peptide Models

Olivia E. Schroeder,[†] Emily Carper,[†] Joshua J. Wind,[†] Jennifer L. Poutsma,*[,‡] Felicia A. Etzkorn,[§] and John C. Poutsma*[,†]

Department of Chemistry, The College of William and Mary, Williamsburg, Virginia, 23187-8795, Department of Chemistry and Biochemistry, Old Dominion University, Norfolk, Virginia 23529-0126, and Department of Chemistry, Virginia Tech, Blacksburg, Virginia 24061-0212

Received: January 30, 2006; In Final Form: March 29, 2006

The energetics of cis−trans proline isomerization in small peptide models have been investigated using the hybrid density functional theory method B3LYP with a 6-31+G* basis set. The molecules studied are models for the phospho-Ser/Thr-Pro substrate for Pin-1, a peptidyl-prolyl isomerase (PPIase) involved in cell division. Pin-1 requires phosphorylation of a Ser or Thr residue adjacent to a Pro residue in the substrate and catalyzes cis−trans isomerization about the proline amide bond. The dihedral angle that would correspond to the reaction coordinate for isomerization of the ω peptide bond was investigated for several small models. Relaxed potential energy scans for this dihedral angle in *N*-methylacetamide, **1**, *N*,*N*-dimethylacetamide, **2**, acetylpyrrolidine, **3** and acetylproline, **4**, were carried out in 20° steps using the B3LYP/6-31+G* level of theory. In addition, similar scans were carried out for **1**−**4** protonated on the acetylamide carbonyl oxygen. Optimized structures for **1**−**4** protonated on the amide nitrogen were also obtained at B3LYP/6-31+G*. Relative proton affinities were determined for each site at various angles along the reaction coordinate for isomerization. The relative proton affinities were anchored to experimental gas phase proton affinities, which were taken from the literature for **1** and **2**, or determined in an electrospray ionization-quadrupole ion trap instrument using the extended kinetic method for **3** and **4**. Proton affinities of 925 ± 10 and 911 ± 12 kJ/mol were determined for **3** and **4**, respectively. These studies suggest that the nitrogen atom in these amides becomes the most basic site in the molecule at a dihedral angle of ca. 130°. In addition, the nitrogen atoms in **2**−**4** are predicted to attain basicities in the range 920−950 kJ/mol, making them basic enough to be the preferred site for hydrogen bonding in the Pin-1 active site, in support of the proposed mechanism for PPIases.

Introduction

Phosphorylation-dependent prolyl isomerization (regulated by peptidyl-prolyl isomerases) is a signaling mechanism that may play an important role in transcription and may act as a regulatory switch.[1] The family of proteins known as peptidyl-prolyl isomerases (PPIases) includes Pin 1, CyP, and FKBP. Pin1 is particularly important in humans for its ability to regulate entry into mitosis, as well as for its ability to regulate proper progression through mitosis.[2] Pin1 isomerizes phosphoSer/Thr-Pro sequences reversibly between cis and trans amide conformations (Scheme 1). The specificity of Pin1 for phosphorylated Ser or Thr is strong, up to 200-fold higher k_{cat}/K_m with phosphorylation in the preferred sequence.[3] Thus, although levels of Pin1 remain constant during the cell cycle, the interaction between the enzyme and its targets is dependent on mitotic phosphorylation of the target proteins.[2]

Mechanistic enzymology in the study of PPIases is limited to studies of CyP and FKBP. PPIase reactions are difficult to examine by traditional mechanistic probes because no bonds are made or broken and no cofactors undergo concomitant change. The cis−trans isomerization (Scheme 1) is typically a slow process because of the partial double bond character of the rotatable amide C−N bond.[4] The problem of this energy barrier is alleviated by the presence of PPIases that help in the isomerization. Three simple mechanisms are chemically sensible: (1) attack by a nucleophile at the amide carbonyl (enzyme thiol or general base), (2) twisting the amide bond out of conjugation (twistase), facilitated by hydrogen-bonding to the prolyl nitrogen (Figure 1), and (3) protonation of the Pro nitrogen (general acid). Each of these represents a way to disrupt the carbon−nitrogen π−bond of the amide and leave it with only a single bond that can rotate. For mechanism 2, the isolation of the amide bond from water may also be important as the amide rotational barrier is ∼3 kcal/mol lower in less polar solvents.[5,6]

SCHEME 1: Isomerization of -pSer-Pro- Amides by Pin1

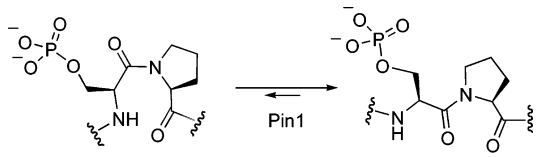

The experimental data available suggest that PPIases accomplish isomerization via mechanism 2. For human cyclophilin A (hCyPA), the nucleophilic catalysis mechanism (1) has been ruled out by mutagenesis of each of four cysteines,[7] and a normal secondary deuterium kinetic isotope effect.[8−10] For both CyP and FKBP a general acid (3) or general base (1) catalyzed

[†] The College of William and Mary.
[‡] Old Dominion University.
[§] Virginia Tech.

10.1021/jp060642u CCC: $33.50
Published on Web 05/04/2006

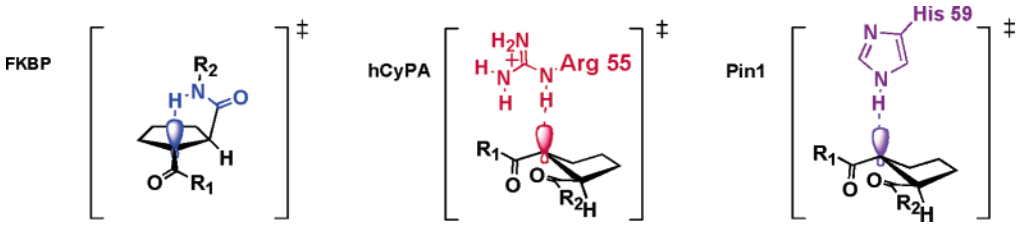

Figure 1. Proposed hydrogen-bond assisted twistase mechanisms for the three families of PPIase.

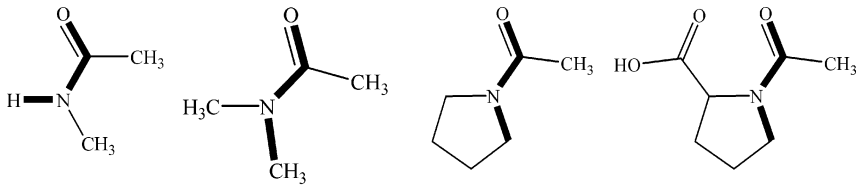

1 **2** **3** **4**

Figure 2. Dipeptide models investigated in the study.

mechanism was ruled out because the enzymatic reaction rate is independent of the pH between 5 and 9, and there is no solvent deuterium isotope effect.[8] In addition, the general acid mechanism (3) is unlikely because the carbonyl oxygen is substantially more basic than the nitrogen of the amide. However, a temporary hydrogen bond or partial proton transfer to the nitrogen would be expected to accelerate the reaction by reducing amide resonance.

The twistase mechanism (2) was proposed on the basis of observations that the ketone carbonyl of the FK506 α-ketoamide was orthogonal to the amide plane in the bound conformation[11,12] and normal secondary kinetic isotope effects for cyclophilin substrates deuterated on the *N*-terminal side of the Xaa-Pro amide.[8,9,13] It has been suggested that PPIases bind Xaa-Pro substrates and distort the amide bond by pyramidalizing the prolyl nitrogen through hydrogen bonding.[4,14] Intramolecular donation of the hydrogen bond from the prolyl *C*-terminal amide in the substrate bound to FKBP was proposed.[4] Nonenzymatic intramolecular catalysis by this mechanism was demonstrated in solution.[15] In hCyPA, we proposed that the active site Arg55 could act as the hydrogen donor because the orientation of the substrate in the hCyPA active site does not allow an intramolecular hydrogen bond.[14,16] The Arg55Ala mutant was enzymatically inactive (1000-fold less than the wild type).[17] The X-ray structure of a tetrapeptide substrate bound to CyP shows nonplanar Xaa-*cis*-Pro amide bonds with angles of 45° and 22° for independent molecules.[16] These results support a mechanism for PPIase enzymatic activity that is a combination of substrate distortion and stabilization by hydrogen bonding to the Pro nitrogen.

Further evidence for mechanism 2 comes from calculations on the reaction path for isomerization by FKBP12.[4] The energy for catalysis comes mainly from substrate destabilization by twisting the amide carbonyl out of plane with nitrogen by 24°. Stabilization of the incipient lone pair on nitrogen by the *substrate* amide proton of the residue *C*-terminal to proline (substrate autocatalysis) comes into play for FKBP. A similar recent calculation of the cyclophilin reaction pathway[18] agrees with our mutagenesis results and in turn supports our hypothesis of a hydrogen bonding role for Arg55 in catalysis.[14,17]

In summary, for cyclophilin and FKBP, the results rule out an enzymatic nucleophile or general base attack at the carbonyl carbon. Theory and experiment support a hydrogen-bond assisted twisted-amide transition state in the CyP and FKBP classes of PPIases. However, this proposed mechanism calls for hydrogen bonding to the proline nitrogen rather than to the more basic carbonyl oxygen. A possible explanation for this is that upon binding in a twisted conformation resonance is disrupted enough for the nitrogen to now be the more basic site. The hydrogen bond will further disrupt resonance decreasing the barrier to rotation. Karplus et al. observed this in their calculations.[4] The barrier for rotation was much lower in energy when the hydrogen bond was to the nitrogen than when the hydrogen bond was to the carbonyl oxygen. This leads to two questions: (1) at what point does the nitrogen become more basic than the carbonyl oxygen and (2) how basic does the nitrogen become?

As an initial investigation into the mechanism for Pin1 and to answer the above questions, we performed combined theoretical/experimental investigations of the nitrogen basicity in small molecule models of the O-phosSer/Thr-Pro substrate of Pin-1. Because the dipeptide substrate is beyond the computational resources of our current laboratory, we chose to study small model compounds, *N*-methylacetamide, **1**, *N*,*N*-dimethylacetamide, **2**, acetylpyrrolidine, **3**, and acetylproline, **4** (Figure 2). The proton affinities of the amide nitrogen atom and amide carbonyl oxygen atom, which are being used as a measure of basicity, were obtained at various points along the cis−trans peptide bond isomerization coordinate. The hybrid density functional theory method B3LYP/6-31+G* was used for all calculations. Relative proton affinities were anchored to experimental proton affinities, which were determined using the entropy-corrected extended kinetic method in an electrospray ionization − quadrupole ion trap mass spectrometer.

Computational and Experimental Methods

Theoretical Procedures. All calculations were performed either on desktop PCs using Gaussian 98W[19] or on multiprocessor servers running RedHat Linux using Gaussian 98. Molecular geometries were first optimized using the hybrid density functional method B3LYP[20,21] and a 6-31+G* basis set. The dihedral angle that would correspond to the cis−trans isomerization reaction coordinate (bold bonds in Figure 2) was then scanned over 360° in 20° steps. At each step, the dihedral angle was frozen and the remaining degrees of freedom were optimized. To eliminate effects of local minima, the scans were repeated in the opposite directions and composite potential energy surfaces were generated using the lowest energy at each dihedral angle as shown in Figure 3. For **4**, additional scans were performed in which the acid carbonyl group was frozen in a position to hydrogen bond to either the amide nitrogen atom

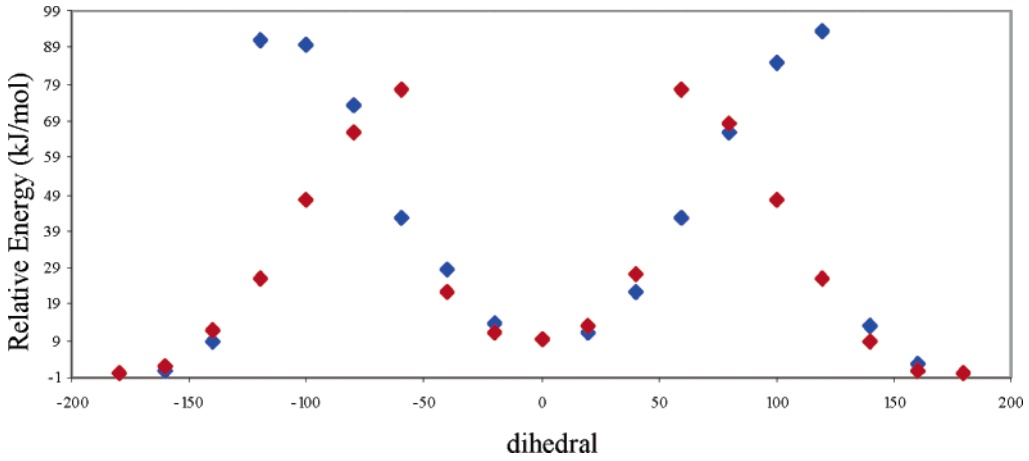

Figure 3. Plot of relative B3LYP/6-31+G* energy for **1** as a function of OCNH bond angle. The red diamonds indicate a scan with step size +20°; the blue diamonds indicate a step size of −20°.

or the amide carbonyl oxygen atom. The lowest energy structure at each dihedral angle was used to form the composite scan for **4**.

The procedure was repeated for the dipeptide models protonated at the amide carbonyl oxygen atom for compounds **1**−**4**. Estimates for the proton affinity at each different site of the peptide models were obtained by subtracting the energy for the protonated model from the energy of the neutral model at each step along the reaction coordinate. Protonation at the nitrogen atom causes a change of hybridization from sp^2 to sp^3, making a direct dihedral comparison with the neutral amide complicated. Therefore, no scan was performed for the protonated nitrogen and the same energy, that of the unconstrained optimized protonated nitrogen structure, was subtracted from each neutral structure along the dihedral scan to obtain the nitrogen proton affinity.

This approach gives poor absolute proton affinity estimates as it neglects zero-point energy and thermal energy effects as well as the contribution from the proton. However, *relative* proton affinities among the different sites should be well represented because of the small difference between ZPE and thermal corrections for the different protonated forms. Relative PAs were calculated for each site and the results were anchored to the experimental PA obtained from the literature or from experiments in the ion trap (see below). The anchor point was assigned to either the 180° (trans in Scheme 1) or 0° (cis in Scheme 1) point for carbonyl oxygen protonation for each model.

Mass Spectrometry. All mass spectrometry experiments were performed on a Finnigan LCQ-DECA quadrupole ion trap instrument with an electrospray ionization source using methods described in detail elsewhere.[22,23] Briefly, proton-bound dimer ions of the form $A-H^+-B_i$, where A is the analyte molecule with unknown proton affinity and B_i is one of a series of reference bases with known proton affinity, were formed by direct infusion of dilute solutions (ca. 5×10^{-4} M) of a mixture of A and B_i in either slightly acidified (1% HOAc) methanol or 50:50 methanol:water. Flow rates were optimized to maximize proton-bound dimer ion production and were on the order of 10−30 μL/min. Ion focusing conditions were also optimized to maximize dimer ion formation. The proton-bound dimer ions were isolated in a first stage of mass spectrometry and were allowed to collide with the background helium buffer gas with nominal lab frame collision energy in the range 0.75−4.25 eV (15−85%) in the laboratory frame. The ratio of the ionic products AH^+ and B_iH^+ resulting from multiple collisions with the helium buffer gas were recorded at each collision energy and were used in an extended kinetic method analysis[24−27] to determine proton affinities.

The extended kinetic method has been reviewed in detail elsewhere[24] and has been used by our group[22,23,28,29] and others[24−26,30−35] in previous studies to obtain both enthalpies of protonation (−PA) and entropies of protonation for a wide variety of molecules. In this study we used the *entropy-corrected* version of the extended kinetic method as developed by Cooks and co-workers.[34] Briefly, the ratios B_iH^+/AH^+ were recorded for a series of *n* reference bases at a given activation energy. A plot (plot 1) of $\{\ln(B_iH^+/AH^+) - \Delta S_p(B_i)\}$ vs $\{PA(B_i) - PA_{avg}\}$, where PA_{avg} is the average proton affinity of the *n* reference bases and $\Delta S_p(B_i)$ is the protonation entropy of the reference base B_i, is generated according to the Armentrout modification[27] of the methods of Fenselau,[25] Wesdemiotis,[26] and Cooks.[34] By convention, the constant entropy of the proton (106 J mol^{-1} K^{-1}) is removed from the protonation entropy.[34] From these data, a best fit line was generated with slope of $1/RT_{eff}$ and intercept of $-\{PA(A) - PA_{avg}\}/RT_{eff} + \Delta S_{p,A}/R$. The procedure was repeated for several different activation energies and separate plots were made for each of the activation energies. The extended kinetic method then required a second plot (plot 2) of the negative intercepts of the best fit lines from plot 1 versus their slopes. The desired proton affinity was obtained from the slope of plot 2 ($PA - PA_{avg}$) and a prediction for the protonation entropy was obtained from the intercept ($\Delta S_{p,A}/R$). The magnitude of the derived entropy term has been the subject of recent debate,[36−40] but the general consensus seems to be that to obtain accurate enthalpies, the extended kinetic method must be used. In this work, the entropy terms are all rather small (<15 J mol^{-1} K^{-1}) and should contribute only minimally to the derived proton affinities.

Materials. Acetylpyrrolidine was synthesized using standard literature procedures.[41] Acetylproline was purchased from Sigma (St. Louis) and was used without further purification. *N*-methylacetamide, *N*,*N*-dimethylacetamide, amine reference compounds and other synthetic materials were purchased from Aldrich and were also used without further purification.

Results and Discussion

As the actual substrate of Pin-1, O-phosSerPro, is beyond the computational resources of our lab at this time, we chose to begin the investigation of the cis−trans peptide bond isomerization with small model compounds, working toward

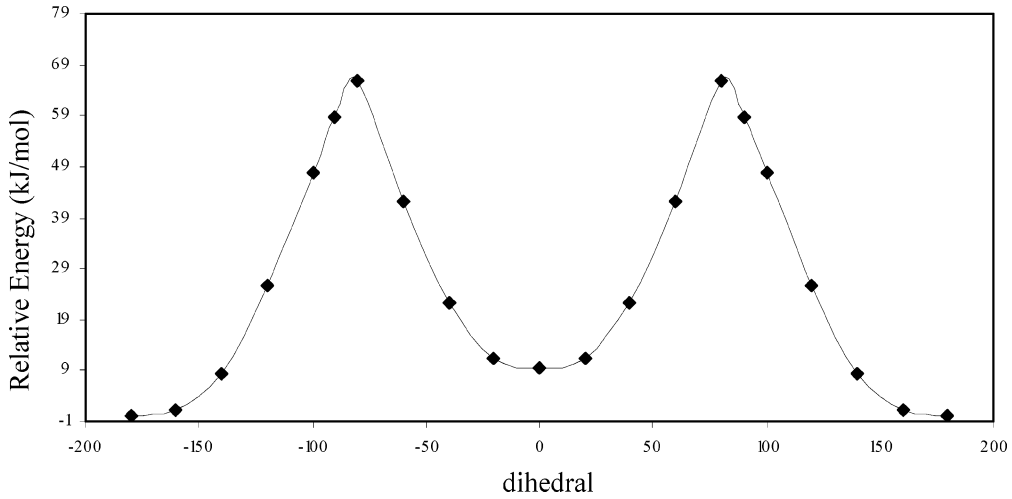

Figure 4. Composite scan (relative E_{elec} (kJ/mol) vs dihedral angle) of forward and reverse dihedral scans for **1**.

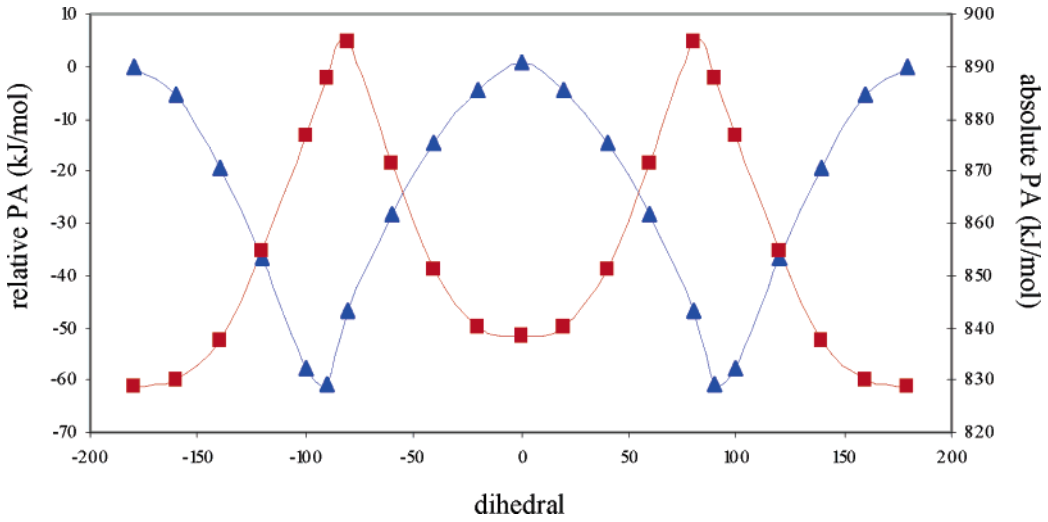

Figure 5. Plot of relative proton affinity (left hand axis) and absolute proton affinity (right hand axis) for carbonyl oxygen protonation (blue triangles) and nitrogen protonation (red squares) of **1** as a function of the OCNH dihedral angle.

the actual dipeptide substrate. Proline is the only amino acid to undergo isomerization, most likely because the energy difference between the cis and trans conformers is the smallest for proline. Typically, proline is found in the cis conformation ($\omega = 0$) in about 10% of proline peptide bonds. However, the fact that proline has two alkyl substituents on the nitrogen versus only one for the other amino acids may also result in a lower barrier for enzyme catalyzed isomerization due to the increased basicity of the nitrogen. Interactions with a hydrogen bond donor will be stronger and the double-bond character of the C−N bond will be further reduced. To investigate this, we begin by comparing *N*-methylacetamide, a model for nonproline amino acids, and *N*,*N*-dimethylacetamide, an acyclic model of proline.

***N*-Methylacetamide, 1.** To investigate the relative basicity of the different sites of *N*-methylacetamide at various points along the reaction coordinate for cis−trans isomerization, relaxed scans were performed using Gaussian 98 using the B3LYP/6-31+G* level of theory. The O−C−N−H (bold bond in Figure 2) dihedral angle was varied in steps of 20° and the rest of the degrees of freedom were allowed to optimize. A plot of the relative electronic energy, E_{elec}, at each dihedral step is shown in Figure 3. Each scan was also run in the opposite direction to eliminate the effects of local minima along the reaction coordinate, also shown in Figure 3. A composite scan of the lowest energy structure at each dihedral angle is generated for each molecule as shown in Figure 4 for *N*-methylacetamide. Composite energies for each neutral model and their oxygen protonated forms at various dihedral angles are presented in Table S1 of the Supporting Information. Total electronic energies for the nitrogen protonated forms are given in Table S2.

A relaxed dihedral scan was also run with **1** protonated on the amide carbonyl oxygen, **1Ha**, and a composite scan was generated, as shown in Figure S1 of the Supporting Information. An optimized geometry was determined for **1** protonated on the amide nitrogen, **1Hb**, and the energy was used to calculate PA as described below. Approximations for the absolute proton affinities at each site can be obtained by subtracting the electronic energy of protonated *N*-methylacetamide from the electronic energy of the neutral *N*-methylacetamide. For **1Ha**, the electronic energies obtained at various dihedral angles were used to calculate PA values, whereas for **1Hb**, the geometry-optimized electronic energy was used at each dihedral step. This approach is obviously crude as it neglects contributions from zero-point energy and thermal corrections as well as the effects of the proton. However, the relative proton affinities among the different protonation sites should be well represented as the *difference* in zero-point energies and thermal corrections for the various protonated forms should be small (Figure 5). As a check, vibrational frequencies were obtained for the 180° dihedral point for **1Ha** and **1Hb**. Zero point energy corrections of 304.3 and 303.6 kJ/mol and thermal corrections of 19.5 and 19.9 kJ/mol

TABLE 1: Absolute Proton Affinities for Amide Nitrogen and Amide Carbonyl Oxygen Atoms in 1−4 at Selected Values of the Dihedral Angle for Cis−Trans Isomerization

	1	2	3	4
min PA nitrogen (dihedral)	827.4 (180)	860.3 (180)	878.9 (180)	866.6 (180)
max PA nitrogen (dihedral)	893.20 (80)	921.8 (80)	947.6 (80)	950.9 (−90)
min PA oxygen (dihedral)	827.5 (90)	838.4 (90)	866.9 (100)	849.7 (90)
max PA oxygen (dihedral)[a]	888.5 (180)	907.9 (180)	925.0 (180)	912.7 (180)[b]

[a] Anchored to experimental PA. [b] See discussion in text about 0° and 40° points.

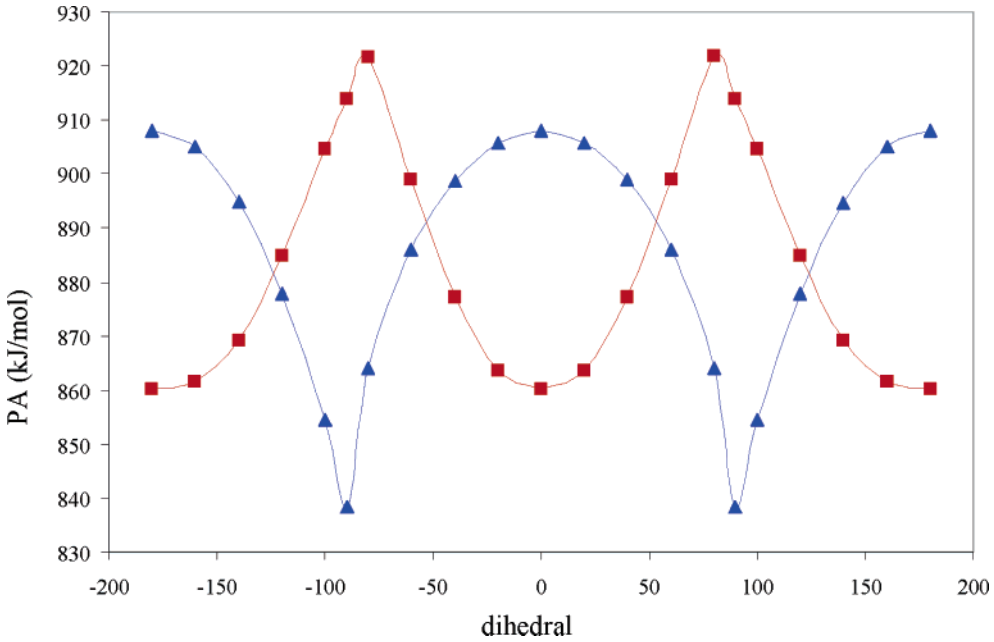

Figure 6. Plot of proton affinity for carbonyl oxygen protonation (blue triangles) and nitrogen protonation (red squares) of **2** as a function of the OCNC dihedral angle.

were found for **1Ha** and **1Hb**, respectively. Correction factors to the electronic energies (ZPE + integrated heat capacity + PV work term) gave 298 K enthalpies for **1Ha** and **1Hb** that differ by less than 0.5 kJ/mol. Given the small differences in these quantities among the different protonated forms, we feel confident in reporting relative proton affinities calculated in this manner.

To obtain a prediction of the basicity of the nitrogen atom at various points along the reaction coordinate, the relative PA values were anchored to the experimental proton affinity of 888.5 kJ/mol.[42] Calculations confirm that the carbonyl oxygen is the most basic site in **1** and that the trans-like conformation is lower in energy than the cis-like conformer. We therefore set the proton affinity of the amide carbonyl oxygen of **1** at 180° to be equal to the experimental value of 888.5 kJ/mol. This method allows for the scale in Figure 5 to be shifted from a relative to absolute scale giving predictions for the PA of the amide nitrogen atom at various points along the cis−trans isomerization coordinate (right-hand axis). Minimum and maximum proton affinities for the amide nitrogen atom and the amide carbonyl oxygen atoms for models **1**−**4** and the respective dihedral angles for these points are given in Table 1. The nitrogen atom becomes the most basic site of the molecule at ∼120° when starting from the trans isomer, and at ∼55° when starting from the cis isomer. The proton affinity of the nitrogen reaches a value of 893 kJ/mol, which is 4.5 kJ/mol higher than the maximum value for the proton affinity of the carbonyl oxygen.

***N*,*N*-Dimethylacetamide, 2.** Similar scans were performed on *N*,*N*-dimethylacetamide, **2**, to investigate the effects of replacing the secondary amide moiety in **1** with a tertiary amide. Plots of energy versus dihedral angle for **2** and O-protonated **2**, **2Ha**, are shown in Figures S2 and S3 in the Supporting Information. As with *N*-methylacetamide, an optimized geometry was obtained for N-protonated **2**, **2Hb**, and was used to predict the PA at the nitrogen atom for **2**.

A proton affinity scan for **2** is shown in Figure 6, with the 180° dihedral point anchored to the gas phase proton affinity for **2** of 908 kJ/mol. As with *N*-methylacetamide, the nitrogen atom in **2** becomes the most basic site at a dihedral angle of ∼125° and ∼55° and attains a PA of 922 kJ/mol. This is 14 kJ/mol more basic than the carbonyl oxygen maximum proton affinity. The addition of the second methyl group has led to several changes. First, the nitrogen is indeed more basic in *N*,*N*-dimethylacetamide than in *N*-methylacetamide by 29 kJ/mol. The more basic nitrogen of *N*,*N*-dimethylacetamide should form a stronger hydrogen bond, which should cause a larger weakening of the C−N double bond character. Note that the basicity of the planar carbonyl oxygen is also increased by 20 kJ/mol by the additional methyl group. Second, the twisted-nitrogen/planar-oxygen proton affinity difference has become significantly larger, mainly because the methyl group had a larger effect on the twisted nitrogen basicity than on the planar oxygen. Thus, there will be less competition between the oxygen and nitrogen in the twisted molecule for hydrogen bonding sites.

Acetylpyrrolidine, 3. To investigate the effects of constraining the amide nitrogen in a ring, we also investigated the nitrogen heterocycle acetylpyrrolidine, **3**. Dihedral scans were performed for acetylpyrrolidine **3** and its oxygen-protonated form, **3Ha**, and are shown in Figures S4 and S5. To anchor the relative proton affinities to an absolute experimental value, the proton affinity of acetylpyrrolidine **3** was redetermined using

TABLE 2: Thermochemical Data for Reference Bases Used in Kinetic Method Experiments

ref	PA (kJ/mol)[a]	$\Delta S/R$[a,b]	**3**	**4**
4-chloropyridine	916.1	0.2405		X
2,5-dimethylpyrrole	918.7	0.3608		X
butylamine	921.5	−0.9622	X	X
pentylamine	923.5	−0.6014	X	X
hexylamine	927.5	−0.6014		X
pyridine	930.0	0.2405		X
exo-2-aminonorbornane	935.3	−0.6014	X	
N,*N*-dimethylaniline	941.1	0.2405	X	

[a] All data taken from refs 42 and 43. [b] Entropy of H^+ removed from ΔS as discussed in the text.

the entropy-corrected extended kinetic method in an electrospray ionization quadrupole ion trap instrument. A value for the PA of **3** of 925.4 kJ/mol is listed on the NIST webbook thermochemistry database.[43] This value was obtained by an ICR equilibrium experiment with ammonia serving as the reference base.[42] We chose to remeasure this value to ensure that the extended kinetic method could accurately predict proton affinities for acetylated nitrogen heterocyclic compounds because we are studying the thermochemical properties of additional nitrogen heterocyles in other studies in our lab for which there have been no experimental PA determinations.

Proton-bound dimer ions of the form $A-H^+-B_i$, where A is the analyte ion and B_i is one of a series of reference bases with known proton affinity, are generated via electrospray ionization of directly infused solution of a mixture of A and B_i in slightly acidified 50:50 H_2O:MeOH. The following reference bases were used in this study: butylamine, pentylamine, exo-2-aminonorbornane, and *N*,*N*-dimethylaniline, with proton affinities listed in Table 2. Figure 7 shows a plot of $\ln[B_iH^+/AH^+]$ vs PA − PA_{avg}, where PA_{avg} is the average proton affinity of the four reference bases used in this study, at three different activation amplitudes. The effective temperature range for these experiments is small due to the relatively low-energy, multiple-collision nature of the ion activation process in the ion trap. A second plot of the negative intercepts of the straight line fits to the data in Figure 7 versus their slopes is shown in Figure 8. The slope of the best-fit line to the data in Figure 8 is −5.2 kJ/mol, which when combined with the average PA for the reference bases of 930.4 kJ/mol gives the desired PA for **3** of 925.1 kJ/mol, in excellent agreement with the previously established value.

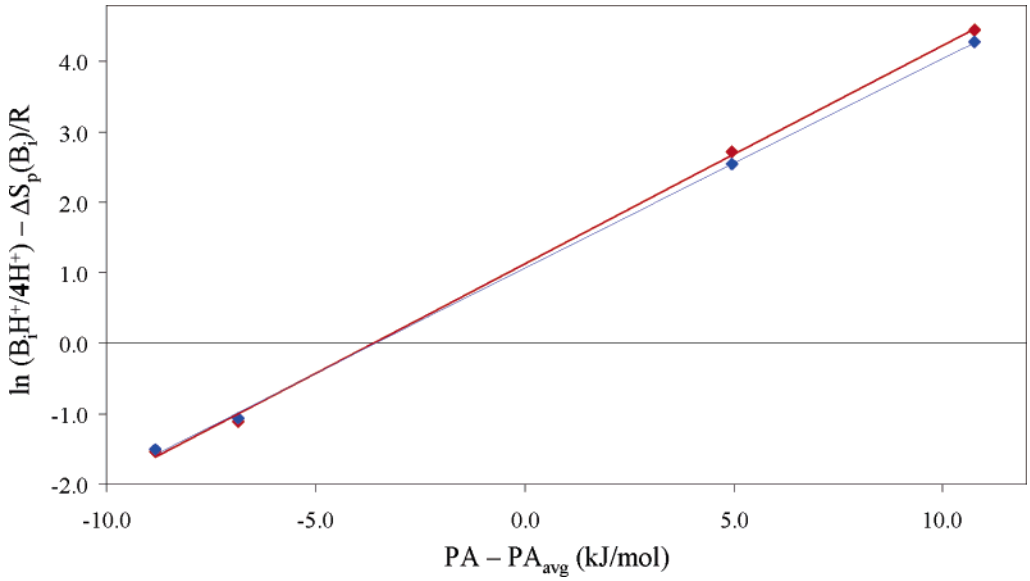

Figure 7. Plot of $\ln(B_iH^+/\mathbf{3}H^+)$ vs $\Delta H_{B_i} - \Delta H_{avg}$ at activation amplitudes 15% (red diamond) and 50% (blue diamond). Data at 25% and 35% not shown for clarity.

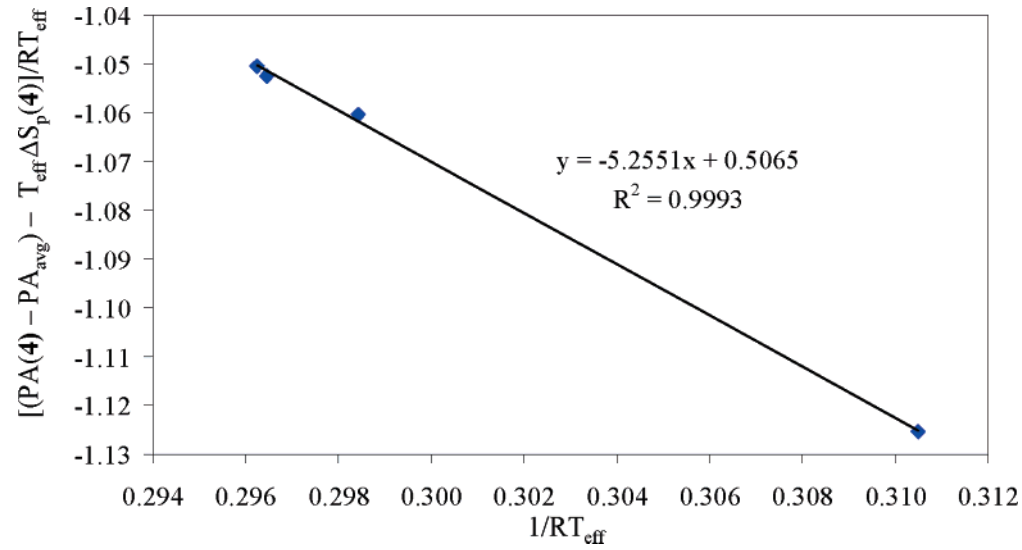

Figure 8. Plot of $[(PA(\mathbf{3}) - PA_{avg}) - T_{eff}\Delta S_p(\mathbf{3})]/RT_{eff}$ vs $1/RT_{eff}$.

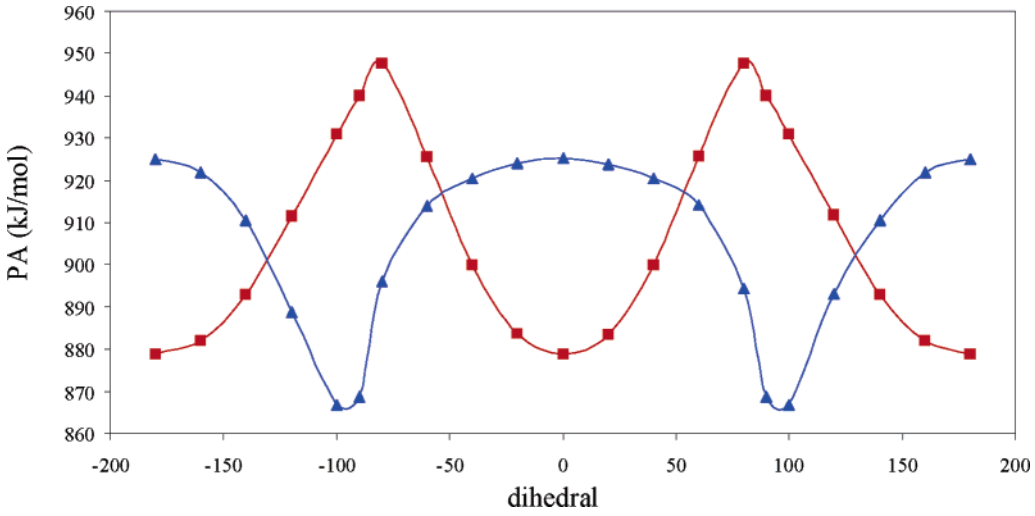

Figure 9. Plot of proton affinity for carbonyl oxygen protonation (blue triangles) and nitrogen protonation (red squares) of **3** as a function of the OCNC dihedral angle.

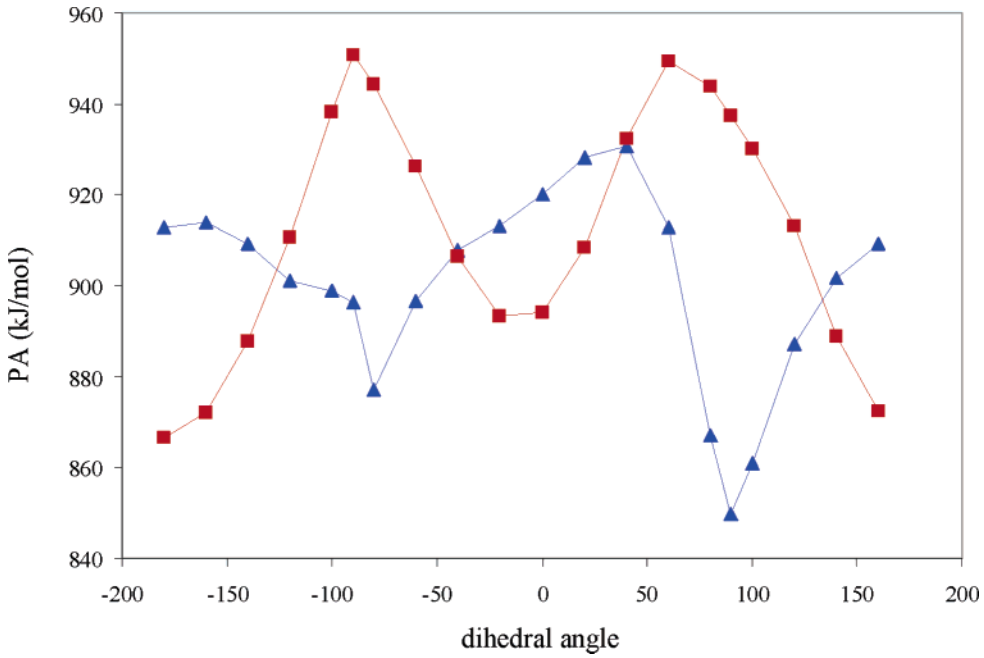

Figure 10. Plot of proton affinity for carbonyl oxygen protonation (blue triangles) and nitrogen protonation (red squares) of **5** as a function of the OCNC dihedral angle.

An alternative way of working up the data involves the use of the new orthogonal distance regression (ODR) technique of Ervin and Armentrout.[38] This technique requires ion ratios for n reference bases at m different activation energies. The program ODR-fit then considers all $n \times m$ points collectively and forces the m different activation energy fits to cross at a single isothermal point. The x-coordinate of this point is $PA - PA_{avg}$ and the y-coordinate is $\Delta S_p/R$. Use of this method avoids making a second kinetic method plot, which can introduce unwanted correlation in the derived data. As such, more realistic error limits can accurately be determined for the derived proton affinity and protonation entropy. In this case, the ODR method gives a PA of 924.4 ± 10 kJ/mol, in excellent agreement with the traditional extended kinetic method results. Entropy contributions in this system were minor, 4 and 5 J mol^{-1} K^{-1} for the traditional and ODR methods of analysis, respectively.

Anchoring the dihedral proton affinity scans to the experimental value of 925.4 kJ/mol leads to the curves shown in Figure 9. As with **1** and **2**, the nitrogen atom becomes the most basic site in the molecule at a dihedral angle of approximately 130° and 55°. More importantly, our calculations predict that the nitrogen atom will attain a proton affinity of 948 kJ/mol. This is 23 kJ/mol higher than the proton affinity for the planar oxygen. The carbonyl oxygen in acetylpyrrolidine is 17 kJ/mol more basic than in *N*,*N*-dimethylactamide and the nitrogen is more than 25 kJ/mol more basic. The addition of the ring has increased both the proton affinity of the nitrogen and the difference in the maximum proton affinities between the twisted nitrogen and planar oxygen. The ring structure causes a slight pyramidalization for the nitrogen (η = 159° for **3** vs 180° for **2**). This reduces the barrier for nitrogen protonation, which results in a sp^3 hybridized nitrogen (η = 123.2° **3Hb** and 122.4° **2Hb**) and increases the barrier for oxygen protonation which prefers a sp^2 hybridized nitrogen (η = 180° **3Ha** and 178° **2Ha**). Overall, this leads to an increase in the difference between the nitrogen and oxygen proton affinities. Thus, proline is better suited than the other amino acids for the twistase mechanism with hydrogen bonding to the nitrogen.

Acetylproline, 4. Dihedral scans were also carried out in a similar manner for acetylproline, **4**. We also attempted to run

dihedral scans with **4** protonated on the carbonyl oxygen in the acid group, **4Hc**; however, during the optimizations, the proton tended to migrate to the amide carbonyl oxygen **4Ha**. This suggests that the proton affinity of the amide carbonyl oxygen is higher than that of the acid carbonyl oxygen, and therefore, we anchored the 180° point of **4Ha** to the experimentally determined value, because the trans conformer is the preferred gas phase structure. Composite scans for **4** and **4Ha** are shown in Figures S6 and S7 in the Supporting Information.

The gas phase PA of **4** was determined in a manner similar to that used to measure the PA for **3**. 4-Chloropyridine, 2,5-dimethylpyrrole, *n*-butylamine, *n*-pentylamine, *n*-hexylamine, and pyridine were used as reference bases (Table 2). Kinetic method plots 1 and 2 for **4** are shown in Figures S8 and S9. The traditional and ODR methods give 912.7 and 910.6 ± 12 kJ/mol for the PA of **4**. Compared to case of proline with a PA of 937 kJ/mol, acetylation lowers the overall PA by 24 kJ/mol.[22] In addition, the PA of the acetyl oxygen is 13 kJ/mol lower than in acetylpyrrolidine. The carbonyl oxygen is most likely less basic for acetylproline because of the hydrogen bond it forms to the OH of the carboxylic acid group.

Anchoring the 180° point for **4Ha** to the gas phase value of 912.7 kJ/mol gives the PA plot shown in Figure 10. The addition of the carboxylic acid group adds an element of asymmetry to the molecule and this is reflected in the scans. Of note is that the amide oxygen is most basic at the 40° point and that the cis conformer is slightly more basic than the trans conformer. The hydrogen bond in the cis compound is between the carboxylic acid OH and the amide nitrogen, which has a smaller effect on the oxygen basicity than the OH−O hydrogen bond in the trans conformer. At the 40° point, neither hydrogen bond is able to attain a short bond length and this leads to the increased basicity of the oxygen.

These scans predict that during the cis−trans isomerization, the nitrogen atom will become as basic as 950 kJ/mol, which is similar to the value obtained for acetylpyrrolidine. The reduced basicity due to the hydrogen bond to the nitrogen atom in the neutral compound is offset by the stabilizing hydrogen bond between the NH and carbonyl oxygen of the carboxylic acid in the nitrogen protonated compound. The difference in basicity between the planar oxygen and twisted nitrogen is now more dramatic at 38 kJ/mol when the PA of the trans conformer is used. However, the difference is only 19 kJ/mol when the maximum PA values for both the nitrogen and oxygen are used, though this value is still large enough to ensure that nitrogen will be the preferred hydrogen bonding site during isomerization.

The nitrogen becomes the preferred spot for protonation at approximately −125°, −40°, +40°, and +135°. These are earlier points along the rotational profile than observed for the other model systems. This means that the enzyme can bind the molecule in a less twisted conformation and still have the nitrogen be the preferred spot for hydrogen bonding. Thus, proline, unlike the other amino acids, is ideally suited for enzymes that use hydrogen bonding to the nitrogen to assist in isomerization.

Supporting Information Available: Tables S1 and S2 of total electronic energy for **1**−**4**, **1Ha**−**4Ha**, and **1Hb**−**4Hb**. Plots of total electronic energy versus dihedral angle for **1Ha**, **2**, **2Ha**, **3**, **3Ha**, **4**, and **4Ha** are available as Figures S1−S7. First and second kinetic method plots for **4** are available as Figures S8 and S9. This material is available free of charge via the Internet at http://pubs.acs.org.

Acknowledgment. Support for this work was provided by the Camille and Henry Dreyfus Foundation, The Thomas F. and Kate Miller Jeffress Memorial Trust, The American Chemical Society Petroleum Research Fund, and the National Science Foundation (CAREER0348889), J.C.P.; the NIH (R01 GM63271), F.A.E.; and Old Dominion University, JP. J.W. and O.S. acknowledge the Howard Hughes Medical Institute for summer fellowships.

References and Notes

(1) Lu, K.; Liou, Y.; Zhou, X. Z. Pinning down proline-directed phosphorylation signaling. *Trends Cell Biol.* **2002**, *12*, 164.

(2) Shen, M.; Stukenberg, P. T.; Kirschner, M. W.; Lu, K. P. The Essential Mitotic Peptidyl-prolyl Isomerase Pin1 Binds and Regulates Mitosis-Specific Phosphoproteins. *Genes Development* **1998**, *12*, 706.

(3) Yaffe, M. B.; Schutkowski, M.; Shen, M.; Zhou, X. Z.; Stukenberg, P. T.; Rahfeld, J. U.; Xu, J.; Kuang, J.; Kirschner, M. W.; Fischer, G.; Cantley, L. C.; Lu, K. P. Sequence-specific and phosphorylation-dependent proline isomerization: a potential mitotic regulatory mechanism. *Science* **1997**, *278* (5345), 1957.

(4) Fischer, S.; Dunbrack, R. L., Jr.; Karplus, M. Cis−Trans Imide Isomerization of the Proline Dipeptide. *J. Am. Chem. Soc.* **1994**, *116* (26), 11931.

(5) Duffy, E. M.; Severance, D. L.; Jorgensen, W. L. Solvent effects on the barrier to isomerization for a tertiary amide from ab initio and Monte Carlo calculations. *J. Am. Chem. Soc.* **1992**, *114*, 7535.

(6) Wiberg, K. B.; Rablen, P. R.; Rush, D. J.; Keith, T. A. Amides. 3. Experimental and Theoretical Studies of the Effect of the Medium on the Rotational Barriers for *N*,*N*-Dimethylformamide and *N*,*N*-Dimethylacetamide. *J. Am. Chem. Soc.* **1995**, *117*, 4261.

(7) Liu, J.; Albers, M. W.; Chen, C.-M.; Schreiber, S. L.; Walsh, C. T. Cloning, expression, and purification of human cyclophilin in *Escherchia coli* and assessment of the catalytic role of cysteines by site-directed mutagenesis. *Proc. Natl. Acad. Sci. U.S.A.* **1990**, *87*, 2304.

(8) Harrison, R. K.; Stein, R. L. Mechanistic Studies of Peptidyl Prolyl Cis−Trans Isomerase: Evidence for Catalysis by Distortion. *Biochemistry* **1990**, *29*, 1684.

(9) Harrison, R. K.; Caldwell, C. G.; Rosegay, A.; Melillo, D.; Stein, R. L. Confirmation of the secondary deuterium isotope effect for the peptidyl prolyl cis−trans isomerase activity of cyclophilin by a competitive, double-label technique. *J. Am. Chem. Soc.* **1990**, *112*, 7063.

(10) Harrison, R. K.; Stein, R. L. Mechanistic Studies of Enzymic and Nonenzymic Prolyl Cis−Trans Isomerization. *J. Am. Chem. Soc.* **1992**, *114* (9), 3463.

(11) Rosen, M. K.; Standaert, R. F.; Galat, A.; Nakatsuka, M.; Schreiber, S. L. Inhibition of FKBP Rotamase Activity by Immunosuppressant FK506: Twisted Amide Surrogate. *Science* **1990**, *248*, 863.

(12) Van Duyne, G. D.; Standaert, R. F.; Karplus, P. A.; Schreiber, S. L.; Clardy, J. Atomic Structure of FKBP−FK506, an Immunophilin-Immunosuppressant Complex. *Science* **1991**, *252*, 839.

(13) Stein, R. L. Mechanism of enzymatic and nonenzymatic prolyl cis−trans isomerization. In *Advances in Protein Chemistry*; Lorimer, G., Ed.; Academic Press: San Diego, 1993; Vol. 44, pp 1−24.

(14) Wiederrecht, G.; Etzkorn, F. A. Immunophilins. In *Perspectives in Drug Discovery and Design*; Sigal, N. H., Wyvratt, M. J., Eds.; ESCOM Science Publishers B.V.: Leiden, The Netherlands, 1994; Vol. 2, pp 57−84.

(15) Cox, C.; Lectka, T. Intramolecular Catalysis of Amide Isomerization: Kinetic Consequences of the 5-NH−Nα Hydrogen Bond in Prolyl Peptides. *J. Am. Chem. Soc.* **1998**, *120*, 10660.

(16) Kallen, J.; Walkinshaw, M. D. The X-ray structure of a tetrapeptide bound to the active site of human cyclophilin A. *FEBS Lett.* **1992**, *300* (3), 286.

(17) Zydowsky, L. D.; Etzkorn, F. A.; Chang, H.; Ferguson, S. B.; Stolz, L. A.; Ho, S. I.; Walsh, C. T. Active Site Mutants of Human Cyclophilin A Separate Peptidyl-Prolyl Isomerase Activity from Cyclosporin A Binding and Calcineurin Inhibition. *Protein Sci.* **1992**, *1*, 1092.

(18) Hur, S.; Bruice, T. C. The Mechanism of Cis−Trans Isomerization of Prolyl Peptides by Cyclophilin. *J. Am. Chem. Soc.* **2002**, *124*, 7303.

(19) Frisch, M. J.; Trucks, G. W.; Schlegel, H. B.; Scuseria, G. E.; Robb, M. A.; Cheeseman, J. R.; Zakrzewski, V. G.; Montgomery, J. A., Jr.; Stratmann, R. E.; Burant, J. C.; Dapprich, S.; Millam, J. M.; Daniels, A. D.; Kudin, K. N.; Strain, M. C.; Farkas, O.; Tomasi, J.; Barone, V.; Cossi, M.; Cammi, R.; Mennucci, B.; Pomelli, C.; Adamo, C.; Clifford, S.; Ochterski, J.; Petersson, G. A.; Ayala, P. Y.; Cui, Q.; Morokuma, K.; Malick, D. K.; Rabuck, A. D.; Raghavachari, K.; Foresman, J. B.; Cioslowski, J.; Ortiz, J. V.; Baboul, A. G.; Stefanov, B. B.; Liu, G.; Liashenko, A.; Piskorz, P.; Komaromi, I.; Gomperts, R.; Martin, R. L.; Fox, D. J.; Keith, T.; Al-Laham, M. A.; Peng, C. Y.; Nanayakkara, N.; Challacombe, M.; Gill, P. M. W.; Johnson, B.; Chen, W.; Wong, M. W.; Andres, J. L.; Gonzalez, C.;

Head-Gordon, M.; Replogle, E. S.; Pople, J. A. *Gaussian 98*, version A.9; Gaussian, Inc: Pittsburgh, PA, 1998.

(20) Becke, A. D. Density Functional Thermochemistry. III. The Role of Exact Exchange. *J. Chem. Phys.* **1993**, *98*, 5648.

(21) Lee, C.; Yang, W.; Parr, R. G. Development of the Colle-Salvetti Correlation Energy Formula into a Functional of the Electron Density. *Phys. Rev. B* **1988**, *37*, 785.

(22) Kuntz, A. F.; Boynton, A. W.; David, G. A.; Colyer, K. E.; Poutsma, J. C. Proton Affinities of Proline Analogs Using the Kinetic Method with Full Entropy Analysis. *J. Am. Soc. Mass Spectrom.* **2002**, *13*, 72.

(23) Schroeder, O. E.; Andriole, E. J.; Carver, K. L.; Poutsma, J. C. The Proton Affinity of Lysine Analogues Using the Extended Kinetic Method. *J. Phys. Chem. A* **2004**, *108*, 326.

(24) Cooks, R. G.; Patrick, J. S.; Kotiaho, T.; McLuckey, S. A. Thermochemical Determinations by the Kinetic Methodol. *Mass Spectrom. Rev.* **1994**, *18*, 287.

(25) Wu, Z.; Fenselau, C. Gas Phase Basicities and Proton Affinities of Lysine and Histidine Measured from the Dissociation of Proton-Bound Dimers. *Rapid Commun. Mass Spectrom.* **1994**, *8*, 777.

(26) Cerda, B. A.; Wesdemiotis, C. The Relative Copper(I) Ion Affinities of Amino Acids in the Gas Phase. *J. Am. Chem. Soc.* **1995**, *117*, 9734.

(27) Armentrout, P. B. Entropy Measurements and the Kinetic Method: A Statistically Meaningful Approach. *J. Am. Soc. Mass Spectrom.* **2000**, *11*, 371.

(28) Poutsma, J. C.; Andriole, E. J.; Sissung, T.; Morton, T. H. cis-1,5-Diaminocyclooctanediamine: The Most Basic Gaseous Primary Diamine? *Chem. Commun.* **2003**, *16*, 2040.

(29) Wind, J. J.; Papp, L. D.; Happel, M.; Hahn, K.; Poutsma, J. C. Proton Affinity of β-Oxalylaminoalanine (BOAA). Incorporation of Direct Entropy Correction into the Single Reference Kinetic Method. *J. Am. Soc. Mass Spectrom.* **2005**, *16*, 1151.

(30) Wang, Z.; Chu, I. K.; Rodriquez, C. F.; Hopkinson, A. C.; Siu, K. W. M. α,ω Diaminoalkanes as Models for Bases that Dicoordinate the Proton: An Evaluation of the Kinetic Method for Estimating Their Proton Affinities. *J. Phys. Chem. A* **1999**, *103*, 8700.

(31) Afonso, C.; Modeste, F.; Breton, P.; Fournier, F.; Tabet, J. C. Proton Affinities of the Commonly Occurring L-Amino Acids by Using Electrospray Ionization-Ion Trap Mass Spectrometry. *Eur. J. Mass Spectrom.* **2000**, *6*, 443.

(32) Lardin, H. A.; Squires, R. R.; Wenthold, P. G. Determination of the Electron Affinities of α- and β-Naphthyl Radicals Using the Kinetic Method with Full Entropy Analysis. The C−H bond Dissociation Energies of Naphthalene. *J. Mass Spectrom.* **2001**, *36*, 607.

(33) Bouchoux, G.; Choret, N.; Berruyer-Penaud. Protonation Thermochemistry of a, w-alkyldiamines in the Gas Phase: A Theoretical Study. *J. Phys. Chem. A* **2001**, *105*, 3989.

(34) Zheng, X.; Cooks, R. G. Thermochemical Determinations by the Kinetic Method with Direct Entropy Corrections. *J. Phys. Chem. A* **2002**, *106*, 9939.

(35) Hahn, I. S.; Wesdemiotis, C. Protonation Thermochemistry of β-Alanine. An Evaluation of the Proton Affinities and Entropies Determined by the Extended Kinetic Method. *Int. J. Mass Spectrom.* **2003**, *222*, 465.

(36) Drahos, L.; Vekey, K. Entropy Evaluation using the Kinetic Method: Is it Feasible. *J. Mass Spectrom.* **2003**, *38*, 1025.

(37) Bouchoux, G.; Sablier, M.; Berruyer-Penaud, F. Obtaining Thermochemical Data by the Extended Kinetic Method. *J. Mass Spectrom.* **2004**, *39*, 986.

(38) Ervin, K. M.; Armentrout, P. B. Systematic and Random Errors in Ion Affinities and Activation Entropies from the Extended Kinetic Method. *J. Mass Spectrom.* **2004**, *39*, 1004.

(39) Wesdemiotis, C. Entropy Considerations in Kinetic Method Experiments. *J. Mass Spectrom.* **2004**, *39*, 998.

(40) Drahos, L.; Peltz, C.; Vekey, K. Accuracy of Enthalpy and Entropy Determination Using the Kinetic Method: Are We Approaching a Consensus? *J. Mass Spectrom.* **2004**, *39*, 1016.

(41) Heyde, C.; Zug, I.; Hartmann, H. A Simple Route to N, N-dialkyl Derivatives of 2-Amino-5-thiophenecarboxylates. *Eur. J. Org. Chem.* **2000**, *19*, 3273.

(42) Hunter, E. P.; Lias, S. G. Evaluated Gas Phase Basicities and Proton Affinities of Molecules: An Update. *J. Phys. Chem. Ref. Data* **1998**, *27*, 3.

(43) Lias, S. G.; Bartmess, J. E.; Liebman, J. F.; Holmes, J. L.; Levin, R. D.; Mallard, W. G. Ion Energetics Data. In *NIST Chemistry Webbook, NIST Standard Reference Database Number 69*; Mallard, W. G., Lindstrom, P. J., Eds.; National Institute of Standards and Technology: Gaithersburg, MD, 20899 (http://webbook.nist.gov), 1999.